DETECTION OF DNA HYBRIDIZATION USING $ZnS:Mn^{2+}$ NANOWIRES/SiO_2 CORE/SHELL NANOCOMPOSITES AND Au NANOPARTICLES

Yue Zhou, Jian Cao*, Lili Yang, Maobin Wei, Xiaoyan Liu, Qianyu Liu, Xin Li, Jinghai Yang

Key Laboratory of Functional Materials Physics and Chemistry of the Ministry of Education, National Demonstration Center for Experimental Physics Education, Jilin Normal University, China; e-mail: caojian_928@163.com

The $ZnS:Mn^{2+}$ nanowires (NWs)/SiO_2 nanocomposites and Au nanoparticles (NPs) were used for the first time as donors and acceptors to detect DNA hybridization basing on the mechanism of fluorescence resonance energy transfer (FRET). The $ZnS:Mn^{2+}$ NWs/SiO_2 core/shell nanocomposites with the average diameter of 25 nm were synthesized by the Stöber method. The Au NPs with the average diameter of 19 nm were prepared by the seed-mediated growth method. The fluorescence intensity of $ZnS:Mn^{2+}$ NWs/SiO_2-dsDNA-Au NPs conjugates decreased extremely compared with that of $ZnS:Mn^{2+}$ NWs/SiO_2-DNA conjugates, indicating that FRET occurred between the $ZnS:Mn^{2+}$ NWs/SiO_2 nanocomposites and Au NPs. When the target DNA sequence was added, the fluorescence intensity was restored. Thus, the selective hybridization of the probe DNA to the target DNA can be used for detecting the target DNA.

Keywords: *$ZnS:Mn^{2+}$ nanowire/SiO_2, Au nanoparticle, fluorescence resonance energy transfer, DNA detection.*

ОБНАРУЖЕНИЕ ГИБРИДИЗАЦИИ ДНК С ПОМОЩЬЮ НАНОКОМПОЗИТОВ НАНОПРОВОЛОКА $ZnS:Mn^{2+}$ (ЯДРО)/SiO_2 (ОБОЛОЧКА) И НАНОЧАСТИЦ ЗОЛОТА

Y. Zhou, J. Cao*, L. Yang, M. Wei, X. Liu, Q. Liu, X. Li, J. Yang

УДК 535.372;620.3;547.963.32

Университет Цзилинь, Чанчунь, 130103, Китай; e-mail: caojian_928@163.com

(Поступила 3 апреля 2018)

Нанокомпозиты в виде нанопроволоки (НП) $ZnS:Mn^{2+}$ с оболочкой SiO_2 и наночастицы (НЧ) золота использованы в качестве доноров и акцепторов для обнаружения гибридизации ДНК методом резонансного переноса энергии флуоресценции (FRET). Нанокомпозиты НП $ZnS:Mn^{2+}$ (ядро)/SiO_2 (оболочка) со средним диаметром 25 нм синтезированы методом Штобера. НЧ Au со средним диаметром 19 нм выращены с использованием затравок. Интенсивность флуоресценции коньюгатов НП $ZnS:Mn^{2+}$/SiO_2–дцДНК–Au-НЧ значительно ниже, чем коньюгатов НП $ZnS:Mn^{2+}$/SiO_2–ДНК, что свидетельствует о наличии FRET между НП $ZnS:Mn^{2+}$/SiO_2 и Au-НЧ. При добавлении последовательности ДНК-мишени интенсивность флуоресценции восстанавливалась. Селективная гибридизация зондовой ДНК с ДНК-мишенью может быть использована для обнаружения ДНК-мишени.

Ключевые слова: *нанопроволока $ZnS:Mn^{2+}$/SiO_2, наночастица Au, резонансный перенос энергии флуоресценции, обнаружение ДНК.*

Introduction. Fluorescence resonance energy transfer (FRET) between donor and acceptor has attracted considerable attention for its potential biological applications, such as DNA or RNA detection, because of its merits, such as safety, simplicity, reliability and high sensitivity [1, 2]. Semiconductor nanocrystals (NCs) can be used for detecting and labeling biomolecules due to their superior optical properties such as size-tunable emission wavelength, narrow emission bandwidth, high luminescence quantum yield, long emission lifetime, and excellent photostability [3]. However, semiconductor NCs such as CdSe, CdTe, etc.

are toxic and cannot be metabolized by the human body. Zn and S are essential elements for human, so that ZnS NCs have wide application prospects in the field of biology. After doping Mn^{2+} ions into the ZnS lattice, a strong yellow-orange emission peak centered at ~583 nm ($^4T_1 \rightarrow {}^6A_1$ transition of Mn^{2+}) with a high quantum yield can be observed [4]. Moreover, embedding the ZnS:Mn^{2+} nanocrystals into SiO_2 can not only increase the fluorescence signal greatly but also enable them to prevent photobleaching [5, 6]. To date, most of the ZnS:Mn^{2+}/SiO_2 core/shell nanostructures are spherical. Reports on one-dimensional core/shell nanostructures are rare. It is well known that Au nanoparticles (NPs) are important fluorescent quenchers with excellent properties, such as stability, nontoxicity, and high extinction coefficient [7]. In this work, we synthesize ZnS:Mn^{2+} nanowires (NWs)/SiO_2 core/shell nanocomposites and Au NPs by the Stöber method and seed-mediated growth method, respectively, which are used as donors and acceptors to detect DNA sequence for the first time. We expect that ZnS:Mn^{2+} NWs/SiO_2 core/shell nanocomposites with excellent optical properties can be used for the effective gene detection.

Experiment. Zinc nitrate, manganese nitrate, thiourea, ethylenediamine (EN), concentrated ammonia aqueous solution (25 %), tetraethyl orthosilicate (TEOS), ethanol, ascorbic acid (AA), chloroauric acid tetrahydrate ($HAuCl_4$), sodium borohydride ($NaBH_4$), silver nitrate ($AgNO_3$), cetyltrimethyl ammonium bromide (CTAB), and thioglycolic acid (MPA) are all analytical grade (Shanghai Chemical Reagents Co.), and they can be used without further purification. N-Hydroxysuccinimide (NHS) and 1-ethyl-3-(3-dimethylaminopropyl)carbodiimide (EDC) are purchased from Sigma Aldrich.

DNA oligonucleotides with the concentration of 100 mM are purchased from Sangon (Shanghai, China), and the sequences are listed as follows:

Sequence 1: 5′-NH_2-TGC AAT AGT AAT CAG

Sequence 2: 5′-SH-CTG ATT ACT ATT GCA TGA GGC CTT

Sequence 3: AAG GCC TCA TGC AAT AGT AAT CAG

Preparation of ZnS:Mn^{2+} NWs/SiO_2 nanocomposites. ZnS:Mn^{2+} NWs used in the current experiment were prepared via the solvothermal method, which was reported in our previous paper [8]. ZnS:Mn^{2+} NWs/SiO_2 nanocomposites were synthesized by the Stöber method. Firstly, 50 ml of absolute alcohol, 1 mL of distilled water, 1.7 mL of aqueous ammonia, and 200 μL of TEOS were injected into a conical flask. Then ZnS:Mn^{2+} NWs and CTAB were added to the foregoing solution, which was continuously stirred for 5 h at room temperature. The resulting nanocomposites were then isolated by centrifugation, washed with deionized water for several times, then dried at 50°C for 4 h.

Preparation of Au NPs. Au NPs were prepared according to the seed-mediated growth method [9]. In brief, the seed solution was prepared by mixing 5 mL of CTAB (0.2 M), 2.5 mL of $HAuCl_4$ (1 mM), and 0.6 mL of $NaBH_4$ (10 mM), which was kept at 30°C for 4 h. Then, 50 ml of CTAB (0.2 M) was mixed with 2 mL of $AgNO_3$ (4 mM), 50 mL of $HAuCl_4$ (1 mM), and 0.75 mL of AA (0.10 M). With continuous stirring, 120 μL of the seed solution was added into the above solution to initiate the growth of the Au NPs. This mixture solution was aged at 30°C for 24 h to ensure the full growth of Au NPs.

Conjugation of ZnS:Mn^{2+} NWs/SiO_2 with DNA oligonucleotides (Sequence 1) [10]. ZnS:Mn^{2+} NWs/SiO_2 nanocomposites were dispersed in 100 mL of deionized water by ultrasonication. MPA was injected into the foregoing solution. The mixture was continuously stirred for 1 h at room temperature. The resulting nanocomposites were washed with phosphate buffer (pH 7.0) and isolated by centrifugation, than redispersed in 3.0 ml of 0.05 M Tris-HCl buffer containing 0.02 M NaCl (pH 7.2). Further, 1.2 mg of EDC and 1.8 mg of NHS were added to the solution and the reaction allowed to proceed for 30 min under stirring. DNA oligonucleotides (Sequence 1) were then added, and the reaction was incubated for 12 h. The resulting solution was centrifuged and washed with 0.05 M Tris-HCl for three times, then resuspended in 3.0 mL of 0.05 M Tris-HCl buffer containing 0.02 M NaCl (pH 7.2). Thus, ZnS:Mn^{2+} NWs/SiO_2-ssDNA-1 were obtained.

Conjugation of Au NPs with DNA oligonucleotides (Sequence 2) [10]. Au NPs were dispersed in the phosphate buffer (pH 7.0). DNA oligonucleotides (Sequence 2) were added to the foregoing solution, which was allowed to react for 16 h at 50°C. Then the saline phosphate buffer (10 mM phosphate buffer containing 2 M NaCl, pH 7.0) was added drop wise to a final salt concentration of 0.1 M NaCl, and the reaction continued for 40 h. To remove the free DNA, the solution was centrifuged and resuspended for several times. Finally, it was dispersed in the 10 mM phosphate buffer containing 0.1 M NaCl (pH 7.0). Thus, Au NPs-ssDNA-2 was obtained.

Detection of the target DNA oligonucleotides (Sequence 3) [10]. The as-prepared ZnS:Mn^{2+} NWs/SiO_2-ssDNA-1 and Au NPs-ssDNA-2 were hybridized in the 0.02 M Tris-HCl buffer containing 0.05 M KCl and 0.005 M $MgCl_2$ (pH 8.0) and incubated at 37 °C for 1 h. The fluorescence spectra of the resulting solution were recorded at 590 nm with excitation of 450 nm. Then, the target DNA oligonucleotides (Sequence 3) were added into the ZnS:Mn^{2+} NWs/SiO_2-dsDNA-Au NPs conjugates, and the fluorescence spectra were also recorded.

The X-ray diffraction (XRD) pattern was obtained on a MAC Science MXP-18 X-ray diffractometer (Japan) at room temperature using a Cu target radiation source (1.5406 Å). The transmission electron micrograph (TEM) image was measured on a JEM-2100 electron microscope. The UV-Vis absorption spectrum was characterized on a UV-3101PC UV spectrometer. The photoluminescence (PL) spectrum was taken on a Renishaw *in Via* micro-PL spectrometer at room temperature (λ_{ex} = 325 nm, He-Cd laser). The fluorescence spectrum (FL) was obtained on a Perkin-Elmer LS55 spectrometer at room temperature.

Results and discussion. The XRD patterns of the ZnS:Mn^{2+} NWs and ZnS:Mn^{2+} NWs/SiO_2 nanocomposites (t = 4 h) can be seen in Fig. 1. For the ZnS:Mn^{2+} NWs (Fig. 1a), all the diffraction peaks can be indexed to the hexagonal wurtzite structure of ZnS (JCPDS No. 36-1450). Note that the full width at half-maximum (FWHM) of the (002) diffraction peak is much narrower than that of the other peaks, indicating a preferential growth orientation along the (002) crystal plane of ZnS, which is further proved by HRTEM. In addition, no diffraction peak coming from Mn^{2+} ions can be detected in Fig. 1, suggesting that the Mn^{2+} ions have replaced the Zn^{2+} sites in ZnS NWs. For the ZnS:Mn^{2+} NWs/SiO_2 nanocomposites (Fig. 1b), the intensity of the diffraction peaks is much lower than that of the ZnS:Mn^{2+} NWs, and the characteristic diffraction peak of amorphous SiO_2 locates at ~20–25° [11], indicating that the ZnS:Mn^{2+} NWs have been packed into the SiO_2 matrix.

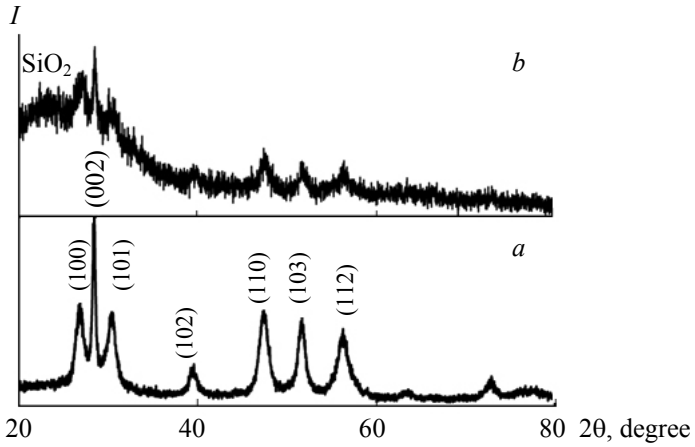

Fig. 1. XRD patterns of the ZnS:Mn^{2+} NWs (a) and ZnS:Mn^{2+} NWs/SiO_2 (b) nanocomposites.

Figure 2 illustrates the TEM, HRTEM, and EDAX images of both the ZnS:Mn^{2+} NWs and ZnS:Mn^{2+} NWs/SiO_2 nanocomposites. The ZnS:Mn^{2+} NWs have a uniform diameter (~8.8 nm) over their entire length (Fig. 2a). From the HRTEM image, the growth direction is perpendicular to the lattice fringes, the d spacing is found to be 0.31 nm (Fig. 2b), corresponding to the (002) plane of wurtzite ZnS [12]. The corresponding SAED is shown in the inset in Fig. 2b. Analysis of the diffraction rings indicates that the ZnS:Mn^{2+} NWs have the wurtzite structure. The EDAX spectrum of the ZnS:Mn^{2+} NWs (Fig. 2c) shows the existence of Zn, S and Mn elements, and the Mn content is about 1.53 at.%, indicating that the Mn^{2+} ions have been incorporated into the ZnS lattice. Figure 2d displays the TEM image of the ZnS:Mn^{2+} NWs/SiO_2 nanocomposites (t = 4 h); the light thin layer corresponding to SiO_2 can be observed around the ZnS:Mn^{2+} NWs, which confirms that the coaxial core/shell structure is composed of the ZnS:Mn^{2+} NWs and SiO_2. Figure 3 displays the typical TEM image of the prepared Au NPs. It can be seen that the Au NPs are monodispersed. Their average diameter is about 19 nm (see inset Fig. 3).

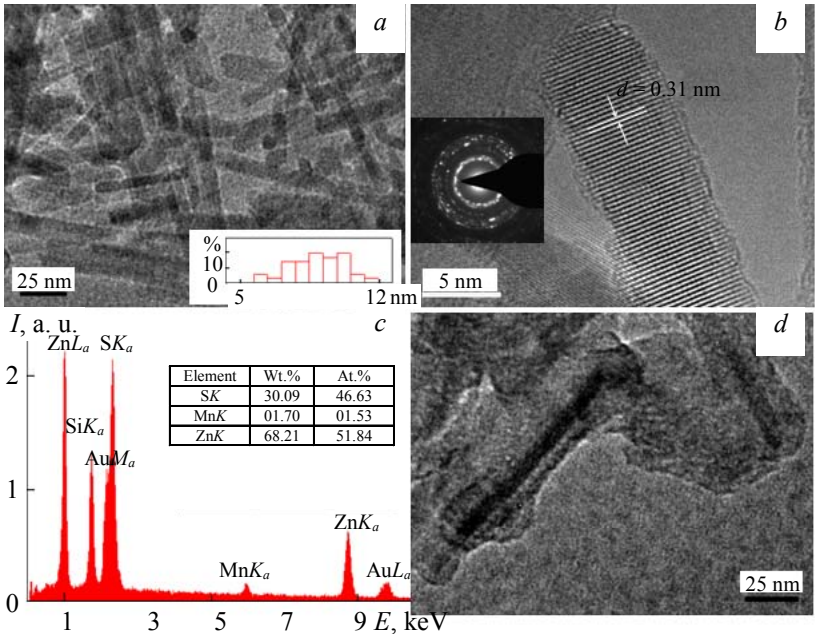

Fig. 2. TEM (a), HRTEM (b), and EDAX (c) images of the ZnS:Mn^{2+} NWs; (d) TEM image of the ZnS:Mn^{2+} NWs/SiO_2 nanocomposites, inset a is the size distribution of the ZnS:Mn^{2+} NWs; inset b is the SAED image of the ZnS:Mn^{2+} NWs.

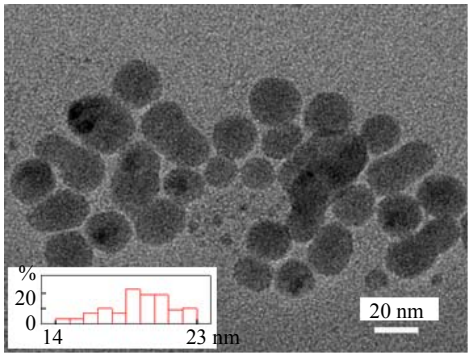

Fig. 3. TEM image of the Au NPs, inset is the size distribution histogram of the Au NPs.

Figure 4 shows the room temperature PL spectra of the ZnS:Mn^{2+} NWs and ZnS:Mn^{2+} NWs/SiO_2 nanocomposites. The PL spectrum of the ZnS:Mn^{2+} NWs exhibits a broad defect-related emission from 400 to 500 nm [13] and a strong yellow orange emission centered at ~584 nm, which is attributed to the efficient energy transfer from the ZnS NWs to Mn^{2+} ions facilitated by the mixed electronic states [14]. Sooklal et al. [15] have found that ZnS with surface bound Mn^{2+} ions leads to the ultraviolet emission, whereas, if the Mn^{2+} ions replaced the Zn^{2+} sites, it would yield the orange emission. So it further proves that the Mn^{2+} ions have been incorporated into the ZnS:Mn^{2+} NWs. For the ZnS:Mn^{2+} NWs/SiO_2 nanocomposites, the intensity of the yellow orange emission keeps increasing until t = 4 h, and decreases gradually when the time increases to 6 h. At the early stage, the surface of the ZnS:Mn^{2+} NWs was passivated fully by SiO_2. So the surface quenching centers would be reduced. As the reaction progresses, the shell thickness of SiO_2 becomes larger, inducing localized strain at the interface, which may be the main reason for the decrease of the yellow-orange emission [16].

Figure 5a exhibits the UV-Vis absorption spectrum of the Au NPs. It can be seen that the absorption band is located at ~520–650 nm, which is consistent with literature [17]. Figure 5b shows the fluorescence spectrum of the ZnS:Mn^{2+} NWs/SiO_2 (t = 4 h) nanocomposites. The emission peak of the ZnS:Mn^{2+} NWs/SiO_2 nanocomposites is located at 594 nm overlapping with the absorption spectrum of the Au NPs. Consequently, the efficient FRET will occur between the ZnS:Mn^{2+} NWs/SiO_2 nanocomposites and Au NPs.

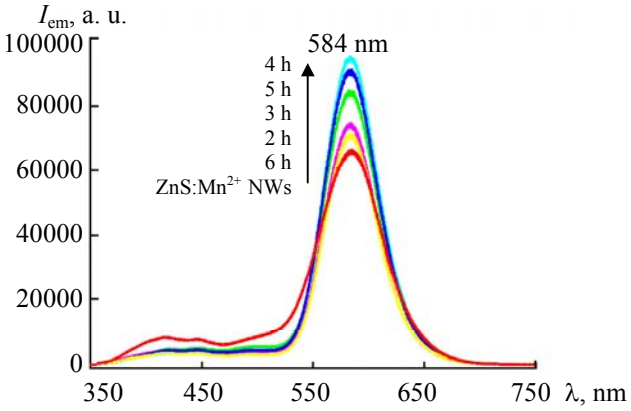

Fig. 4. PL spectra of the ZnS:Mn^{2+} (3%) NWs and ZnS:Mn^{2+} NWs (3%)/SiO_2 nanocomposites under different hydrolysis times of TEOS.

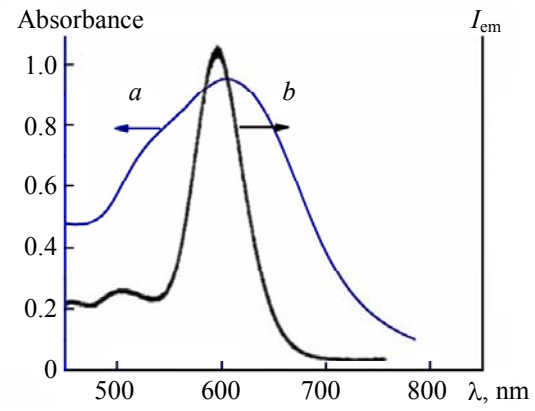

Fig. 5. Absorption spectrum of the Au NPs (a) and the emission spectrum of the ZnS:Mn^{2+} NWs/SiO_2 nanocomposites (b).

Figure 6 is a schematic illustration of FRET between the ZnS:Mn^{2+} NWs/SiO_2-ssDNA-1 and Au NPs-ssDNA-2. When the ZnS:Mn^{2+} NWs/SiO_2-ssDNA-1 mix with Au-ssDNA-2, the hybridization between DNA sequences 1 and 2 will lead to the contact of the ZnS:Mn^{2+} NWs/SiO_2 nanocomposites and Au NPs. Consequently, the fluorescence of the ZnS:Mn^{2+} NWs/SiO_2 nanocomposites will be quenched by the Au NPs based on the FRET mechanism. After adding the target DNA sequence 3, the fluorescence of the ZnS:Mn^{2+} NWs/SiO_2 nanocomposites is restored. Thus, the selective hybridization of the probe DNA to the target DNA will turn the fluorescence on, which can be used to detect the target DNA.

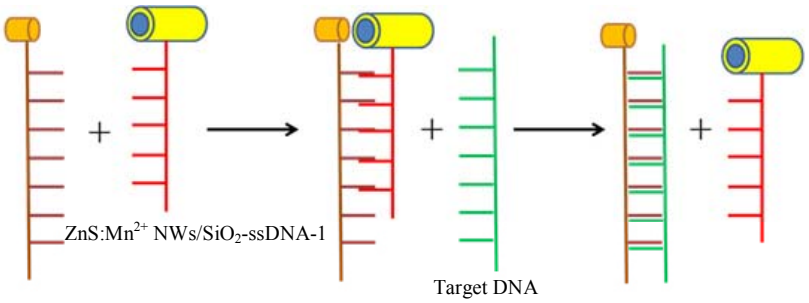

Sequence 1: 5′-NH_2-TGC AAT AGT AAT CAG
Sequence 2: 5′-SH-CTG ATT ACT ATT GCA TGA GGC CTT
Sequence 3: AAG GCC TCA TGC AAT AGT AAT CAG

Fig. 6. Schematic illustration of DNA detection based on FRET mechanism between the ZnS:Mn^{2+} NWs/SiO_2-ssDNA-1 and Au NPs-ssDNA-2.

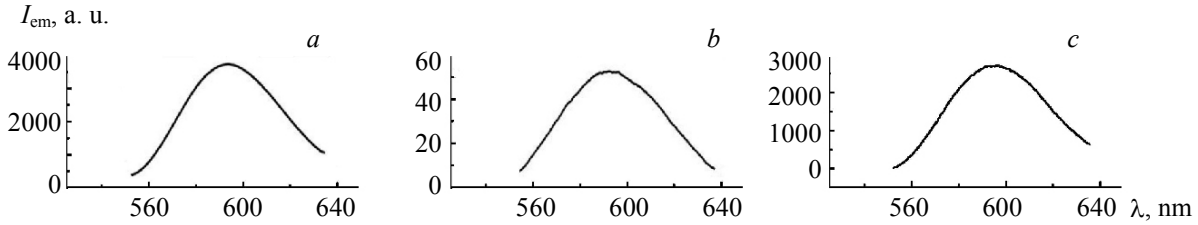

Fig. 7. Fluorescence spectra of the ZnS:Mn^{2+} NWs/SiO_2-ssDNA-1 (a), ZnS:Mn^{2+} NWs/SiO_2-dsDNA-Au (b), and ZnS:Mn^{2+} NWs/SiO_2-dsDNA-Au with the complementary target DNA (sequence 3) (c) under the same excitation of 450 nm.

Figure 7a shows the FL spectrum of the ZnS:Mn^{2+} NWs/SiO_2-ssDNA-1. There is a strong yellow orange emission peak centered at 594 nm. After adding the Au NPs-ssDNA-2, the emission intensity is quenched and is 70 times lower than that of the ZnS:Mn^{2+} NWs/SiO_2-ssDNA-1 (Fig. 7b). When the target DNA is added, the fluorescence intensity is restored (Fig. 7c), since the target DNA has more complementary bases to the sequence 2 than sequence 1. The ZnS:Mn^{2+} NWs/SiO_2-ssDNA-1 will be released, resulting in the recovered fluorescence.

Conclusion. The ZnS:Mn^{2+} NWs/SiO_2 nanocomposites were used as donor to detect the specific DNA sequence based on the FRET mechanism for the first time. FRET occurred when the ZnS:Mn^{2+} NWs/SiO_2-ssDNA-1 and Au NPs-ssDNA-2 were in close proximity to each other after hybridization. After adding the target DNA into this probe system, the fluorescence intensity was increased.

Acknowledgment. This work was supported by the National Natural Science Foundation of China (No. 61705079, 61475063), the National Key Research and Development Program of China (Grant No. 2017YFF0108607).

REFERENCES

1. E. Oh, M. Hong, D. Lee, S. Nam, H. C. Yoon, H. Kim, *J. Am. Chem. Soc.*, **127**, 3270–3271 (2005).
2. X. Hu, X. Zhang, W. Jin, *Electrochim. Acta*, **94**, 367–373 (2013).
3. A. P. Alivisatos, *Science*, **271**, 933–937 (1996).
4. L. Liu, L. Xiao, H. Zhu, *Chem. Phys. Lett.*, **539**, 112–117 (2012).
5. H. L. Ding, Y. X. Zhang, S. Wang, J. M. Xu, S. C. Xu, G. H. Li, *Chem. Mater.*, **24**, 4572–4580 (2012).
6. A. Fu, W. Gu, B. Boussert, K. Koski, D. Gerion, L. Manna, M. L. Gros, C. A. Larabell, A. P. Alivisatos, *Nano Lett.*, **7**, 179–182 (2007).
7. B. Dubertret, M. Calame, A. J. Libchaber. *Nat. Biotechnol.*, **19**, 365–370 (2001).
8. J. Cao, B. Wang, D. Han, S. Yang, Q. Liu, T. Wang, H. Niu, J. Yang, *Materials Lett.*, **135**, 71–74 (2014).
9. B. Nikoobacht, M. A. E. Sayed, *Chem. Mater.*, **15**, 1957–1962 (2003).
10. F. Gao, P. Cui, X. Chen, Q. Ye, M. Li, L. Wang, *Analyst*, **136**, 3973–3980 (2011).
11. J. Cao, H. Niu, D. Han, S. Yang, Q. Liu, T. Wang, J. Yang, *J. Mater. Sci: Mater. Med.*, **26**, 236–242 (2015).
12. S. Biswas, S. Kar, S. Chaudhuri, *J. Phys. Chem. B*, **109**, 17526–17530 (2005).
13. M. V. Limaye, S. Gokhale, S. A. Acharya, S. K. Kulkarni, *Nanotechnology*, **19**, 415602–415607 (2008).
14. R. N. Bhargava, D. Gallagher, X. Hong, A. Nurmikko, *Phys. Rev. Lett*, **72**, 416–419 (1994).
15. K. Sooklal, B. S. Cullum, S. M. Angel, C. J. Murphy, *J. Phys. Chem.*, **100**, 4551–4555 (1996).
16. J. Cao, J. H. Yang, L. L. Yang, M. B. Wei, B. Feng, D. L. Han, L. Fan, B. J. Wang, H. Fu, *J. Appl. Phys.*, **112**, 014316–014324 (2012).
17. F. Kim, J. H. Song, P. Yang, *J. Am. Chem. Soc.*, **124**, 14316–14317 (2002).